

An Orthogonal Basis Approach to Formation Shape Control (Extended Version) ^{*}

Tairan Liu ^a, Marcio de Queiroz ^b

^a*School of Electrical and Computer Engineering, University of Georgia, Athens, GA 30602, USA*

^b*Department of Mechanical and Industrial Engineering, Louisiana State University, Baton Rouge, LA 70803, USA*

Abstract

In this paper, we propose a novel approach to the problem of augmenting distance-based formation controllers with a secondary constraint for the purpose of preventing 3D formation ambiguities. Specifically, we introduce three controlled variables that form an orthogonal space and uniquely characterize a tetrahedron formation in 3D. This orthogonal space incorporates constraints on the inter-agent distances and the signed volume of tetrahedron substructures. The formation is modeled using a directed graph with a leader-follower type configuration and single-integrator dynamics. We show that the proposed decentralized formation controller ensures the *global* asymptotic stability and the local exponential stability of the desired formation for an n -agent system with no ambiguities. Unlike previous work, this result is achieved without conditions on the tetrahedrons that form the desired formation or on the control gains.

Key words: Formation Control; Orthogonal Basis; Distance; Signed Volume.

1 Introduction

In formation shape control, a group of interacting mobile agents are commanded to acquire and maintain a desired geometric pattern in space. A well-known method for solving this problem involves regulating a set of inter-agent distances to values prescribed by the desired shape (de Queiroz et al.; 2019; Krick et al.; 2009). This method, which is commonly referred to as distance-based formation control (Oh et al.; 2015), has the main advantage of being implementable in a fully decentralized manner. However, this advantage comes with the limitation that the set of inter-agent distances may not uniquely define the formation position and orientation in space. Mathematically, this nonuniqueness is related to the existence of multiple equilibrium points in the multi-agent system distance dynamics. The question then is how do you steer the system away from the undesired equilibria and towards the equilibrium corresponding to the desired formation shape (up to translation and rotation).

The above question is partially answered by requiring the formation graph to be rigid, which imposes a minimum number of distances to be controlled. This reduces the unwanted equilibrium points to formations that are flipped or reflected versions of the desired shape. Here, the agents' initial conditions determine whether the formation converges to one that is isomorphic to the desired formation or to a flipped/reflected formation. This implies that rigid distance-based controllers are locally stable.

In recent years, some methods have been introduced to address the limitation of distance-based formation controllers. The common feature of these methods is the use of an additional controlled variable (or constraint) that is capable of distinguishing formation ambiguities. In Mou et al. (2015), an approach called target-point control was introduced to rule out the undesirable equilibria in planar formations. The inter-agent distances and the order of agents were used to calculate the desired position of the agents, i.e., target position, in a local coordinate frame. However, the leader and the first follower cannot be collocated at time zero and the leader's motion needs to satisfy certain conditions. A similar method was used in Kang et al. (2017) with the name "desired order of neighbors". In Ferreira-Vazquez, Hernandez-Martinez, Flores-Godoy, Fernandez-Anaya

^{*} This paper is the extended version of our paper submitted to Automatica with the proof of some lemmas. Corresponding author M. de Queiroz. Tel. +1-225-578-8770.

Email addresses: Tairan.Liu@uga.edu (Tairan Liu), mdeque1@lsu.edu (Marcio de Queiroz).

and Paniagua-Contro (2016), inter-agent distance and angular constraints were employed to enlarge the region of attraction to the desired planar formation by a proper choice of control gains. In Anderson et al. (2017), the signed area of a triangle was used as the second controlled variable, and convergence analyses were conducted for special cases of 3- and 4-agent planar formations. In Sugie et al. (2018), the authors further explored the idea of Anderson et al. (2017) by applying the area constraints to only a subset of agents and thus extended the method to n agents. However, the result in Sugie et al. (2018) required the triangulated formation to be composed of equilateral triangles. Recently in Liu et al. (n.d.), we extended the distance/signed area method to directed 2D formations of n agents and introduced the concept of strong congruency. In this result, the triangulations were not restricted to equilateral ones; however, certain triangulation and control gain conditions had to be met to prove the asymptotic stability of the desired formation. In Cao et al. (2019), a specific control gain value in the signed area term was found that causes the multi-agent system to have one stable equilibrium point corresponding to the desired formation and some discrete unstable equilibria. A switching control strategy based on the signed area or edge angle was proposed in Liu, Fernández-Kim and de Queiroz (2020) to remove the restrictions on the shape of the desired formation. In Liu and de Queiroz (n.d.), we designed a non-switching, distance/edge angle-based controller that ensures the almost-global asymptotic stability of the desired formation under certain conditions on the triangulations. Recently in Jing and Wang (2020), a formation controller based on angles and the “sign” of the triangulated framework was shown to guarantee almost-global convergence of the angle errors.

For the 3D formation problem, relatively few results exist. For example, Ferreira-Vazquez, Flores-Godoy, Hernandez-Martinez and Fernandez-Anaya (2016) extended the method in Ferreira-Vazquez, Hernandez-Martinez, Flores-Godoy, Fernandez-Anaya and Paniagua-Contro (2016) to 3D by using distance and volume constraints. However, unless the control gains satisfy a persistency of excitation-type condition, the system under the control of Ferreira-Vazquez, Flores-Godoy, Hernandez-Martinez and Fernandez-Anaya (2016) may still converge to an undesired formation shape. In Lan et al. (2018), volume constraints were applied to a 4-agent system to distinguish the two possible orientations of a tetrahedron under the assumption that three of the agents are at their desired distances.

In this paper, we address the problem of using additional feedback variables in the distance-based 3D formation controller. Specifically, we introduce a new method called the *orthogonal basis approach* which decomposes the feedback variables and control inputs into three orthogonal subspaces. By applying this decomposition to directed frameworks formed by tetrahedrons, we are

able to guarantee the *global* asymptotic stability of the desired formation. Moreover, we can show the desired formation is locally exponentially stable which provides robustness to the system. These results are achieved with no limitations on the “tetrahedralizations” of the desired formation, control gains, or number of agents. Thus, this work greatly extends the applicability of the dual-feedback-variable approach for avoiding 3D formation ambiguities. To the best of our knowledge, it is the first result to show convergence to the desired 3D formation for all initial conditions, including collocated and collinear agents. A preliminary version of our orthogonal basis approach appeared in Liu, de Queiroz and Sahebsara (2020), where it was applied to planar formations and achieved almost-global asymptotic stability of the desired formation.

2 Background Material

Some background material is reviewed in this section. Throughout the paper, we use the following vector notation: $x \in \mathbb{R}^n$ or $x = [x_1, \dots, x_n]$ denotes an $n \times 1$ (column) vector, and $x = [x_1, \dots, x_n]$ where $x_i \in \mathbb{R}^m$ is the stacked $mn \times 1$ vector.

2.1 Graph Theory

An undirected graph G is represented by a pair $(\mathcal{V}, \mathcal{E}^u)$, where $\mathcal{V} = \{1, 2, \dots, N\}$ is the set of vertices and $\mathcal{E}^u = \{(i, j) | i, j \in \mathcal{V}, i \neq j\} \subset \mathcal{V} \times \mathcal{V}$ is the set of undirected edges. A directed graph G is a pair $(\mathcal{V}, \mathcal{E}^d)$ where the edge set \mathcal{E}^d is directed in the sense that if $(i, j) \in \mathcal{E}^d$ then i is the source vertex of the edge and j is the sink vertex. The set of neighbors of vertex $i \in \mathcal{V}$ is defined as $\mathcal{N}_i(\mathcal{E}^d) = \{j \in \mathcal{V} | (i, j) \in \mathcal{E}^d\}$. For $i \in \mathcal{V}$, the out-degree of i (denoted by $\text{out}(i)$) is the number of edges in \mathcal{E}^d whose source is vertex i and sinks are in $\mathcal{V} - \{i\}$. If $p_i \in \mathbb{R}^3$ is the coordinate of the i th vertex of a 3D graph, then a framework F is defined as the pair (G, p) where $p = [p_1, \dots, p_N] \in \mathbb{R}^{3N}$.

Let the map $\mathcal{T} : \mathbb{R}^3 \rightarrow \mathbb{R}^3$ be such that $\mathcal{T}(x) = \mathcal{R}x + d$ where $\mathcal{R} \in SO(3)$ and $d \in \mathbb{R}^3$. A framework $F = (G, p)$ is rigid in \mathbb{R}^3 if all of its continuous motions satisfy $p_i(t) = \mathcal{T}(p_i)$ for all $i = 1, \dots, N$ and $\forall t \geq 0$ (Asimov and Roth; 1979; Izestiev; 2009). A 3D rigid framework is minimally rigid if and only if $|\mathcal{E}^u| = 3N - 6$ (Anderson et al.; 2008). The edge function of a minimally rigid framework $\gamma : \mathbb{R}^{3N} \rightarrow \mathbb{R}^{3N-3(3+1)/2}$ is defined as

$$\gamma(p) = [\dots, \|p_i - p_j\|, \dots], (i, j) \in \mathcal{E}^u \quad (1)$$

such that its l th component, $\|p_i - p_j\|$, relates to the l th edge of \mathcal{E}^u connecting the i th and j th vertices. Frameworks (G, p) and (G, \hat{p}) are equivalent if $\gamma(p) = \gamma(\hat{p})$, and are congruent if $\|p_i - p_j\| = \|\hat{p}_i - \hat{p}_j\|$ for all distinct vertices i and j in \mathcal{V} (Jackson; 2007). If rigid frameworks

(G, p) and (G, \hat{p}) are equivalent but not congruent, they are flip- or flex-ambiguous (Anderson et al.; 2008).

Frameworks based on directed graphs are required to be constraint consistent and persistent to maintain its shape (Yu et al.; 2007). A persistent graph is said to be minimally persistent if no single edge can be removed without losing persistence. A sufficient condition for a directed graph $(\mathcal{V}, \mathcal{E}^d)$ in \mathbb{R}^3 to be constraint consistent is $\text{out}(i) \leq 3$ for all $i \in \mathcal{V}$ (see Lemma 5 of Yu et al. (2007)). A necessary condition for a graph in \mathbb{R}^3 to be minimally persistent is $\text{out}(i) \leq 3$ for all $i \in \mathcal{V}$, while a sufficient condition is minimal rigidity (Yu et al.; 2007). A minimally persistent graph can be constructed by the 3D Henneberg insertion of type I¹ (Grasegger et al.; 2018). This method starts with three vertices with three directed edges, and grows the graph by iteratively adding a vertex with three outgoing edges. Henceforth, we refer to a framework constructed in this manner as a 3D Henneberg framework.

2.2 Strong Congruency

The concept of congruency defined above can distinguish between two frameworks that are flip- or flex-ambiguous, but does not capture a third type of ambiguity — a reflection of the whole framework. In Liu et al. (n.d.), we introduced the concept of *strong congruency* to handle this type of ambiguity in 2D. Specifically, Henneberg frameworks $F = (G, p)$ and $\hat{F} = (G, \hat{p})$ are said to be *strongly congruent* if they are congruent and not reflected versions of each other.

In Liu et al. (n.d.) (Lemma 2.2), it was shown that the signed area of a triangular framework in addition to a set of edge lengths can be used to ensure strong congruency in 2D. In order to extend this concept to 3D, we will employ the *signed volume of a tetrahedron*, $V : \mathbb{R}^{12} \rightarrow \mathbb{R}$ (Mallison; 1935):

$$\begin{aligned} V(p) &= \frac{1}{6} \det \begin{bmatrix} 1 & 1 & 1 & 1 \\ p_1 & p_2 & p_3 & p_4 \end{bmatrix} \\ &= -\frac{1}{6} (p_1 - p_4)^\top [(p_2 - p_4) \times (p_3 - p_4)] \end{aligned} \quad (2)$$

where $p = [p_1, p_2, p_3, p_4]$. If the order of vertices 1, 2, 3 is counterclockwise (resp., clockwise) from an observer located at vertex 4 facing the 1-2-3 plane, then (2) is positive (resp., negative). Moreover, this quantity is zero if any three vertices are collinear or the four vertices are coplanar. As an example of the use of the signed volume, all the frameworks in Figure 1 are congruent, but only frameworks (a), (b), and (c) are strongly congruent.

¹ As shown in Grasegger et al. (2018), the 3D Henneberg insertion of type I does not allow edge splitting operations (Eren et al.; 2005) in the graph construction procedure.

Hereafter, we denote the set of all 3-dimensional frameworks that are strongly congruent to framework F by $\text{SCgt}^3(F)$.

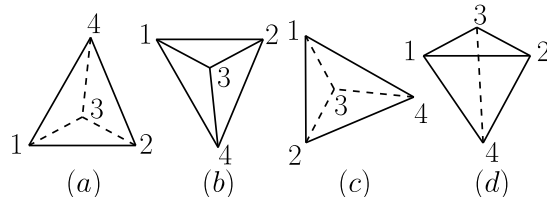


Fig. 1. All four 3D frameworks are congruent, but only the ones in (a), (b), and (c) are strongly congruent.

A 3D Henneberg framework can be divided into tetrahedral sub-frameworks. In such cases, the signed volume of a 3D Henneberg framework with N vertices and directed edge set \mathcal{E}^d , $\mathbf{V} : \mathbb{R}^{3N} \rightarrow \mathbb{R}^{N-3}$, is defined as

$$\begin{aligned} \mathbf{V}(p) &= \left[\dots, \frac{1}{6} \det \begin{bmatrix} 1 & 1 & 1 & 1 \\ p_i & p_j & p_k & p_l \end{bmatrix}, \dots \right], \\ \forall (l, i), (l, j), (l, k) &\in \mathcal{E}^d - \{(2, 1), (3, 1), (3, 2)\} \end{aligned} \quad (3)$$

where $p = [p_1, \dots, p_N]$ and its n th component is the signed volume of the n th tetrahedron constructed with vertices $i < j < k < l$. For example, the signed volume of the framework in Figure 2 is given by

$$\mathbf{V}(p) = \left[\begin{aligned} &-\frac{1}{6} (p_1 - p_4)^\top [(p_2 - p_4) \times (p_3 - p_4)] \\ &-\frac{1}{6} (p_1 - p_5)^\top [(p_3 - p_5) \times (p_4 - p_5)] \end{aligned} \right] \quad (4)$$

where the first element is positive and the second one negative. Note that if \hat{F} is a reflected version of F , then $\mathbf{V}(p) = -\mathbf{V}(\hat{p})$.

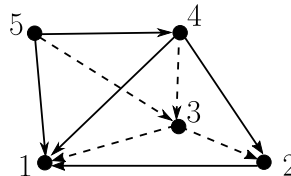


Fig. 2. Framework with two tetrahedrons.

Lemma 1 *3D Henneberg frameworks $F = (G, p)$ and $\hat{F} = (G, \hat{p})$ are strongly congruent if and only if they are equivalent and $\mathbf{V}(p) = \mathbf{V}(\hat{p})$. (See Appendix A.1 for proof.)*

2.3 Stability Results

Here, we recall some results concerning the stability of nonlinear systems.

Lemma 2 (Khalil; 2015) Suppose $f(x, u)$ is continuously differentiable and globally Lipschitz in $[x, u]$. If $\dot{x} = f(x, 0)$ has a globally exponentially stable (GES) equilibrium point at the origin, then the system $\dot{x} = f(x, u)$ is input-to-state stable (ISS).

Lemma 3 (Khalil; 2015) If the systems $\dot{\eta} = f_1(\eta, \xi)$ and $\dot{\xi} = f_2(\xi, u)$ are ISS, then the cascade connection

$$\dot{\eta} = f_1(\eta, \xi), \quad \dot{\xi} = f_2(\xi, u) \quad (5)$$

is ISS. Consequently, if $\dot{\eta} = f_1(\eta, \xi)$ is ISS and the origin of $\dot{\xi} = f_2(\xi, 0)$ is globally asymptotically stable (GAS), then the origin of the cascade connection

$$\dot{\eta} = f_1(\eta, \xi), \quad \dot{\xi} = f_2(\xi, 0) \quad (6)$$

is GAS.

3 Problem Statement

Consider a system of mobile agents described by directed framework $F(t) = (G, p(t))$ where $G = (\mathcal{V}, \mathcal{E})$, $|\mathcal{V}| = N$, $|\mathcal{E}| = 3N - 6$, $N \geq 4$, $p = [p_1, \dots, p_N]$, and $p_i \in \mathbb{R}^3$ is the position of agent i . The directed edge $(j, i) \in \mathcal{E}$ means that agent j can measure its relative position to agent i , $p_{ji} := p_i - p_j$, but not the opposite. We assume agent j can sense all relative positions p_{ji} where $i \in \mathcal{N}_j(\mathcal{E})$. The agents are assumed to be governed by the dynamics

$$\dot{p}_i = u_i, \quad \forall i \in \mathcal{V} \quad (7)$$

where $u_i \in \mathbb{R}^3$ is the control input.

The desired formation is characterized by a set of desired distances d_{ji} , $(j, i) \in \mathcal{E}$ and a set of desired signed volumes $V_{ijkl}^* = V(p_i^*, p_j^*, p_k^*, p_l^*)$, $(l, i), (l, j), (l, k) \in \mathcal{E}$ (see (2)) where p_i^* is the desired position of agent i .² This gives the desired framework $F^* = (G, p^*)$ where $p^* = [p_1^*, \dots, p_N^*]$ and $\|p_j^* - p_i^*\| = d_{ji}$. We assume F^* satisfies the following conditions: i) F^* is non-degenerate in 3D space, i.e., all tetrahedrons have nonzero volume; ii) $\text{out}(i) = i - 1$ for $i = 1, 2, 3$ and $\text{out}(i) = 3$ for $i = 4, \dots, N$; and iii) if there is an edge between agents i and j , the direction must be $i \leftarrow j$ if $i < j$. Given these conditions, we say that agent 1 is the leader, agent 2 is the first follower, agent 3 is the secondary follower, and agents $i \geq 4$ are ordinary followers. Note that this nomenclature is the 3D extension of the leader-first-follower, minimally persistent framework discussed in Summers et al.

² Note that p_i^* is not explicitly used by the control since we are not controlling the global position of the agents. This variable is only mentioned so we can formally define the desired formation.

(2011), which was called an acyclic minimally structural persistent framework in Lan et al. (2018).

Our control objective is to design $u_i, \forall i \in \mathcal{V}$ such that

$$F(t) \rightarrow \text{SCgt}^3(F^*) \text{ as } t \rightarrow \infty \quad (8)$$

for the largest set of initial conditions possible.

4 Orthogonal Basis

Ambiguous frameworks in 3D can be discerned by employing the signed volume of the framework in the formation controller. However, this variable may introduce new undesired equilibria since the distance and volume constraints will interfere with each other at certain agent positions. In other words, these two variables do not always constitute an orthogonal space. To remedy this situation, we will introduce projection variables that are always orthogonal.

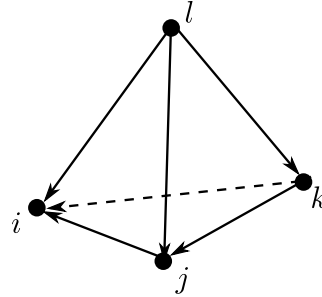


Fig. 3. Tetrahedron framework.

Consider the tetrahedron in Figure 3. If $\|p_{ji}\| \neq 0$ and if there exists a vector n_{ijk} such that

$$n_{ijk}^\top p_{ki} = 0 \quad \text{and} \quad n_{ijk}^\top p_{kj} = 0, \quad (9)$$

then $p_{ji}^\top n_{ijk} = 0$, $p_{ji}^\top (n_{ijk} \times p_{ji}) = 0$, $n_{ijk}^\top (n_{ijk} \times p_{ji}) = 0$, and we say $\{p_{ji}, n_{ijk} \times p_{ji}, n_{ijk}\}$ is the *orthogonal basis of vertex l*. With this in mind, the projection variables for vertex l are defined as

$$\zeta_l = p_{li}^\top p_{ji} = \|p_{li}\|^2 - p_{li}^\top p_{lj} \quad (10a)$$

$$\varphi_l = p_{li}^\top (n_{ijk} \times p_{ji}) = p_{lj}^\top (n_{ijk} \times p_{ji}) \quad (10b)$$

$$\vartheta_l = p_{li}^\top n_{ijk} = p_{lj}^\top n_{ijk} = p_{lk}^\top n_{ijk}, \quad (10c)$$

where

$$n_{ijk} = \begin{cases} p_{ki} \times p_{kj}, & \text{if } \{i, j, k\} \neq \{1, 2, 3\} \\ \frac{p_{31} \times p_{32}}{\|p_{31} \times p_{32}\|}, & \text{if } \{i, j, k\} = \{1, 2, 3\} \\ & \text{and } \|p_{31}(t) \times p_{32}(t)\| \neq 0 \\ n_{123}^+, & \text{if } \{i, j, k\} = \{1, 2, 3\} \\ & \text{and } \|p_{31}(0) \times p_{32}(0)\| = 0 \end{cases} \quad (11)$$

and n_{123}^+ is any unit vector satisfying $p_{31}^\top n_{123}^+ = 0$ and $p_{32}^\top n_{123}^+ = 0$. This unit vector can be computed using Algorithm 1 below. Notice that (10a) (resp., (10b); (10c)) is associated with the projection of p_{li} onto the direction of p_{ji} (resp., $n_{ijk} \times p_{ji}$; n_{ijk}). The reason for differentiating $\{i, j, k\} = \{1, 2, 3\}$ from the case $\{i, j, k\} \neq \{1, 2, 3\}$ in (11) is that our framework is composed of multiple tetrahedrons where vertices $\{1, 2, 3\}$ have different out-degree properties than the others (see Section 3).

Algorithm 1 Selecting n_{123} when $\|p_{31}(0) \times p_{32}(0)\| = 0$. (The value $1e - 3$ below can be replaced with any sufficiently small number.)

```

1: Input:  $p_{31} = [x_1, y_1, z_1], p_{32} = [x_2, y_2, z_2]$ 
2: Output:  $n_{123}$ 
3:  $\text{eps} \leftarrow 1e - 3$ 
4: if  $\|p_{31}\| > \text{eps}$  then
5:   if  $|z_1| > \text{eps}$  then
6:      $n_z \leftarrow -(x_1 + y_1) / z_1$ 
7:      $n_t \leftarrow [1, 1, n_z]$ 
8:   else if  $|y_1| > \text{eps}$  then
9:      $n_y \leftarrow -(x_1 + z_1) / y_1$ 
10:     $n_t \leftarrow [1, n_y, 1]$ 
11:   else if  $|x_1| > \text{eps}$  then
12:      $n_x \leftarrow -(y_1 + z_1) / x_1$ 
13:      $n_t \leftarrow [n_x, 1, 1]$ 
14:   end if
15: else if  $\|p_{32}\| > \text{eps}$  then
16:   if  $|z_2| > \text{eps}$  then
17:      $n_z \leftarrow -(x_2 + y_2) / z_2$ 
18:      $n_t \leftarrow [1, 1, n_z]$ 
19:   else if  $|y_2| > \text{eps}$  then
20:      $n_y \leftarrow -(x_2 + z_2) / y_2$ 
21:      $n_t \leftarrow [1, n_y, 1]$ 
22:   else if  $|x_2| > \text{eps}$  then
23:      $n_x \leftarrow -(y_2 + z_2) / x_2$ 
24:      $n_t \leftarrow [n_x, 1, 1]$ 
25:   end if
26: else
27:    $n_t \leftarrow [0, 0, 1]$ 
28: end if
29:  $n_{123} \leftarrow n_t / \|n_t\|$ 

```

Generally, the above projection variables are defined for agents $l \geq 4$ since a tetrahedron is composed of four

vertices and only agents $l \geq 4$ have $\text{out}(l) = 3$. Therefore, special definitions for the projection variables are required for agents 2 and 3. For agent 2, we define

$$\zeta_2 = p_{21}^\top n_2, \quad (12)$$

where

$$n_2 = \begin{cases} \frac{p_{21}}{\|p_{21}\|}, & \text{if } \|p_{21}(t)\| \neq 0 \\ n_2^+, & \text{if } \|p_{21}(0)\| = 0 \end{cases} \quad (13)$$

and n_2^+ is any unit vector. Variables φ_2 and ϑ_2 are undefined since $\text{out}(2) = 1$. For agent 3, we let $l = k = 3$, $i = 1$, and $j = 2$ in (10a) and (10b) to obtain

$$\zeta_3 = p_{31}^\top p_{21} = \|p_{31}\|^2 - p_{31}^\top p_{32} \quad (14)$$

and

$$\varphi_3 = p_{31}^\top (n_{123} \times p_{21}). \quad (15)$$

Here, variable ϑ_3 is undefined since $\text{out}(3) = 2$.

Remark 1 One can show that projection variable (10c) is related to the signed volume of a tetrahedron and the area of a triangle. Consider (10c) when $\{i, j, k\} \neq \{1, 2, 3\}$. It follows from (11) that

$$\begin{aligned} \vartheta_l &= p_{li}^\top n_{ijk} = p_{li}^\top (p_{ki} \times p_{kj}) \\ &= p_{li}^\top (p_{ki} \times p_{kj}) - p_{ki}^\top (p_{ki} \times p_{kj}) = p_{li}^\top (p_{ki} \times p_{kj}) \\ &= p_{lk}^\top [(p_{li} - p_{lk}) \times (p_{lj} - p_{lk})] \\ &= p_{lk}^\top [p_{li} \times p_{lj} - p_{li} \times p_{lk} - p_{lk} \times p_{lj} + p_{lk} \times p_{lk}] \\ &= p_{lk}^\top (p_{li} \times p_{lj}) = p_{li}^\top (p_{lj} \times p_{lk}) = -6V_{ijkl} \end{aligned} \quad (16)$$

where $V_{ijkl} := V(p_i, p_j, p_k, p_l)$ from (2). When $\{i, j, k\} = \{1, 2, 3\}$ and $\|p_{31} \times p_{32}\| \neq 0$, we have

$$\vartheta_l = p_{l1}^\top n_{123} = \frac{p_{l1}^\top (p_{31} \times p_{32})}{\|p_{31} \times p_{32}\|} = -\frac{3V_{123l}}{\check{S}_{123}} \quad (17)$$

where \check{S}_{ijk} is the regular (unsigned) area of Δ_{ijk} (Heron's formula (Zwillinger; 2002)):

$$\begin{aligned} \check{S}_{ijk} &= \frac{1}{2} \|p_{ki} \times p_{kj}\| \\ &= \frac{1}{4} \left(2 \|p_{ji}\|^2 \|p_{ki}\|^2 + 2 \|p_{ji}\|^2 \|p_{kj}\|^2 \right. \\ &\quad \left. + 2 \|p_{ki}\|^2 \|p_{kj}\|^2 - \|p_{ji}\|^4 - \|p_{ki}\|^4 - \|p_{kj}\|^4 \right)^{1/2}. \end{aligned} \quad (18)$$

The projection variables of a tetrahedralized Henneberg framework (G, p) with $|\mathcal{V}| = N$ is defined as

$$\Lambda(p) = [\Lambda_2, \Lambda_3, \Lambda_4, \dots, \Lambda_N] \quad (19)$$

where

$$\begin{aligned}\Lambda_2 &= \zeta_2 \\ \Lambda_3 &= [\zeta_3, \varphi_3] \\ \Lambda_4 &= [\zeta_4, \varphi_4, \vartheta_4] \\ &\vdots \\ \Lambda_N &= [\zeta_N, \varphi_N, \vartheta_N].\end{aligned}\quad (20)$$

Lemma 4 *3D Henneberg frameworks $F = (G, p)$ and $\hat{F} = (G, \hat{p})$ are strongly congruent if and only if $\Lambda(p) = \Lambda(\hat{p})$. (See Appendix A.2 for proof.)*

Note that by Lemma 4, the control objective in (8) is equivalent to

$$\Lambda(p(t)) \rightarrow \Lambda(p^*) \text{ as } t \rightarrow \infty. \quad (21)$$

5 Formation Controller

5.1 Error Variables

The control objective will be quantified by the following three projection error variables

$$\tilde{\zeta}_l = \zeta_l - \zeta_l^* \quad (22a)$$

$$\tilde{\varphi}_l = \varphi_l - \varphi_l^* \quad (22b)$$

$$\tilde{\vartheta}_l = \vartheta_l - \vartheta_l^* \quad (22c)$$

where the asterisk denotes the desired value for the projection. Since F^* is typically specified in terms of the desired inter-agent distances, the desired projections can be calculated in terms of d_{ji} , $(j, i) \in \mathcal{E}$ as shown in Appendix B. The stacked vector of all the projection errors is represented by $\tilde{\Lambda} = [\tilde{\Lambda}_2, \tilde{\Lambda}_3, \dots, \tilde{\Lambda}_N]$ where $\tilde{\Lambda}_2 = \tilde{\zeta}_2$, $\tilde{\Lambda}_3 = [\tilde{\zeta}_3, \tilde{\varphi}_3]$, and $\tilde{\Lambda}_i = [\tilde{\zeta}_i, \tilde{\varphi}_i, \tilde{\vartheta}_i]$ for $i = 4, \dots, N$.

Lemma 5 *For agent l , the planes corresponding to $\tilde{\zeta}_l = 0$, $\tilde{\varphi}_l = 0$, and $\tilde{\vartheta}_l = 0$ are mutually orthogonal if $\|p_{ji}\| = d_{ji}$, $\|p_{ki}\| = d_{ki}$, and $\|p_{kj}\| = d_{kj}$, where $i < j < k < l$ and $(l, i), (l, j), (l, k) \in \mathcal{E}$. (See Appendix A.3 for proof.)*

5.2 Control Law

We propose the following formation control

$$u_1 = 0 \quad (23a)$$

$$u_2 = \mu_2 \tilde{\zeta}_2 n_2 \quad (23b)$$

$$u_3 = \mu_3 \tilde{\zeta}_3 (p_{31} - p_{32}) + \nu_3 \tilde{\varphi}_3 n_{123} \times (p_{31} - p_{32}) \quad (23c)$$

$$\begin{aligned}u_l &= \mu_l \tilde{\zeta}_l (p_{li} - p_{lj}) + \nu_l \tilde{\varphi}_l n_{ijk} \times (p_{li} - p_{lj}) \\ &\quad + \lambda_l \tilde{\vartheta}_l m_{ijk}, \quad l = 4, \dots, N\end{aligned} \quad (23d)$$

where $i < j < k < l$, $(l, i), (l, j), (l, k) \in \mathcal{E}$, and μ_l, ν_l, λ_l are positive control gains.

Note that since $p_{ki} = p_{li} - p_{lk}$ and $p_{kj} = p_{lj} - p_{lk}$ (see Figure 3), the term n_{ijk} defined in (11) can be expressed as a function of p_{li} , p_{lj} , and p_{lk} for $(l, i), (l, j), (l, k) \in \mathcal{E}$. Therefore, the above control is decentralized in the sense that it requires each agent to know its relative position to neighboring agents only. This means that control (23) can be implemented in each agent's local coordinate frame.

Remark 2 *Since a 3D minimally persistent graph has $3N - 6$ edges, a 3D formation requires $3N - 6$ constraints to maintain its shape. Previous 3D formation control work that utilized distance and volume variables (Ferreira-Vazquez, Flores-Godoy, Hernandez-Martinez and Fernandez-Anaya; 2016) are over-constrained since they require $3N - 6$ distance constraints and $N - 3$ volume constraints. Although these extra constraints rule out formation ambiguities, they introduce new undesired equilibria. On the other hand, the orthogonal basis method proposed here has $N - 1$ ζ -type projection constraints, $N - 2$ φ -type projection constraints, and $N - 3$ ϑ -type projection constraints, totalling exactly $3N - 6$ constraints.*

5.3 Preliminary Analysis

In preparation for our main results, we present next some preliminary results.

Lemma 6 *With control (23), $\dot{n}_2 = 0$ and $\dot{n}_{123} = 0$.*

Proof. If $\|p_{21}\| \neq 0$, the time derivative of (13) is given by

$$\begin{aligned}\dot{n}_2 &= \frac{1}{\|p_{21}\|} (\dot{p}_1 - \dot{p}_2) - \frac{p_{21}}{\|p_{21}\|^2} \frac{d}{dt} \|p_{21}\| \\ &= \frac{1}{\|p_{21}\|} (\dot{p}_1 - \dot{p}_2) - \frac{p_{21}}{\|p_{21}\|^2} \frac{p_{21}^\top (\dot{p}_1 - \dot{p}_2)}{\|p_{21}\|} \\ &= -\frac{1}{\|p_{21}\|} u_2 + \frac{p_{21}}{\|p_{21}\|^3} p_{21}^\top u_2.\end{aligned}\quad (24)$$

After substituting (23) into (24), we obtain

$$\begin{aligned}\dot{n}_2 &= -\frac{1}{\|p_{21}\|} \left(\mu_2 \tilde{\zeta}_2 \frac{p_{21}}{\|p_{21}\|} \right) + \frac{p_{21}}{\|p_{21}\|^3} p_{21}^\top \left(\mu_2 \tilde{\zeta}_2 \frac{p_{21}}{\|p_{21}\|} \right) \\ &= -\mu_2 \tilde{\zeta}_2 \frac{p_{21}}{\|p_{21}\|^2} + \mu_2 \tilde{\zeta}_2 \frac{p_{21}}{\|p_{21}\|^2} \\ &= 0.\end{aligned}\quad (25)$$

When $\|p_{21}\| = 0$, it is obvious from (13) that $\dot{n}_2 = 0$.

If $\|p_{31} \times p_{32}\| \neq 0$, the derivative of (11) is given by

$$\begin{aligned} \dot{n}_{123} &= \frac{1}{\|p_{31} \times p_{32}\|} \frac{d}{dt} (p_{31} \times p_{32}) \\ &\quad - (p_{31} \times p_{32}) \frac{(p_{31} \times p_{32})^\top}{\|p_{31} \times p_{32}\|^3} \frac{d}{dt} (p_{31} \times p_{32}) \end{aligned} \quad (26)$$

where

$$\frac{d}{dt} (p_{31} \times p_{32}) = (u_1 - u_3) \times p_{32} + p_{31} \times (u_2 - u_3). \quad (27)$$

Substituting (23) into (27) yields

$$\begin{aligned} &\frac{d}{dt} (p_{31} \times p_{32}) \\ &= - (p_{31} - p_{32}) \times \left(\mu_3 \tilde{\zeta}_3 p_{21} + \nu_3 \tilde{\varphi}_3 n_{123} \times p_{21} \right) \\ &\quad + p_{31} \times \left(\mu_2 \tilde{\zeta}_2 n_2 \right) \\ &= -\nu_3 \tilde{\varphi}_3 \|p_{21}\|^2 n_{123} + \mu_2 \tilde{\zeta}_2 p_{31} \times n_2. \end{aligned} \quad (28)$$

Since $\|p_{31} \times p_{32}\| \neq 0$, we have

$$\|p_{31} \times p_{32}\| = \|p_{31} \times (p_{31} - p_{21})\| = \|p_{31} \times p_{21}\| \neq 0,$$

which implies $\|p_{21}\| \neq 0$. Then, we can substitute the first case of (13) and the second case of (11) into (28) to obtain

$$\begin{aligned} &\frac{d}{dt} (p_{31} \times p_{32}) \\ &= -\nu_3 \tilde{\varphi}_3 \|p_{21}\|^2 \frac{p_{31} \times p_{32}}{\|p_{31} \times p_{32}\|} + \mu_2 \tilde{\zeta}_2 p_{31} \times \frac{p_{21}}{\|p_{21}\|} \\ &= -\nu_3 \tilde{\varphi}_3 \|p_{21}\|^2 \frac{p_{31} \times p_{32}}{\|p_{31} \times p_{32}\|} - \mu_2 \tilde{\zeta}_2 \frac{p_{31} \times p_{32}}{\|p_{21}\|}. \end{aligned} \quad (29)$$

Now, substituting (29) into (26) gives

$$\begin{aligned} \dot{n}_{123} &= \frac{1}{\|p_{31} \times p_{32}\|} \\ &\quad \cdot \left(-\nu_3 \tilde{\varphi}_3 \|p_{21}\|^2 \frac{p_{31} \times p_{32}}{\|p_{31} \times p_{32}\|} - \mu_2 \tilde{\zeta}_2 \frac{p_{31} \times p_{32}}{\|p_{21}\|} \right) \\ &\quad - (p_{31} \times p_{32}) \cdot \frac{(p_{31} \times p_{32})^\top}{\|p_{31} \times p_{32}\|^3} \left(-\nu_3 \tilde{\varphi}_3 \|p_{21}\|^2 \right. \\ &\quad \left. \cdot \frac{p_{31} \times p_{32}}{\|p_{31} \times p_{32}\|} - \mu_2 \tilde{\zeta}_2 \frac{p_{31} \times p_{32}}{\|p_{21}\|} \right) \\ &= 0. \end{aligned} \quad (30)$$

For $p_{31} \times p_{32} = 0$, it is clear from (11) that $\dot{n}_{123} = 0$. \square

Remark 3 The purpose of n_2^+ in (13) is to force agent 2 to leave the collocated initial position with agent 1. Since $\dot{n}_2 = 0$, the two cases of (13) have the same value. For example, assume the two agents are collocated at time zero and let $n_2^+ = [1, 0, 0]$. Control (23b) will cause agent 2 to move away from the collocated position along vector $[1, 0, 0]$. Since the agents are no longer collocated, then $\frac{p_{21}}{\|p_{21}\|} = [1, 0, 0]$. The vector n_{123}^+ in (11) serves a similar purpose, viz., to force agent 3 to leave the collinear initial position with agents 1 and 2. Note that the second and third cases of (11) have the same value due to $\dot{n}_{123} = 0$. If the three agents are collinear at time zero on the x - y plane and $n_{123}^+ = [0, 0, 1]$ for example, then the second term in (23c) will cause agent 3 to move on the x - y plane away from the collinear position.

Lemma 7 For the two-agent system $\{1, 2\}$, (23a) and (23b) render $\tilde{\zeta}_2 = 0$ GES.

Proof. The time derivative of $\tilde{\zeta}_2$ is given by

$$\dot{\tilde{\zeta}}_2 = (\dot{p}_1 - \dot{p}_2)^\top n_2 + p_{21}^\top \dot{n}_2. \quad (31)$$

Applying Lemma 6 and substituting (23a) and (23b) into (31), we obtain

$$\dot{\tilde{\zeta}}_2 = -n_2^\top u_2 = -\mu_2 \tilde{\zeta}_2 \|n_2\|^2 = -\mu_2 \tilde{\zeta}_2 \quad (32)$$

which indicates that $\tilde{\zeta}_2 = 0$ is GES. \square

Now, consider the Lyapunov function candidates

$$W_3 = \frac{1}{2} \tilde{\zeta}_3^2 + \frac{1}{2} \tilde{\varphi}_3^2 \quad (33a)$$

$$W_l = \frac{1}{2} \tilde{\zeta}_l^2 + \frac{1}{2} \tilde{\varphi}_l^2 + \frac{1}{2} \tilde{v}_l^2, \quad l = 4, \dots, N \quad (33b)$$

where $i < j < k < l$, (l, i) , (l, j) , $(l, k) \in \mathcal{E}$.

Lemma 8 If $\|p_{21}\| = d_{21}$ and $u_2 = 0$, then (23a) and (23c) render $\tilde{\Lambda}_3 = 0$ GES for the three-agent system $\{1, 2, 3\}$.

Proof. The dynamics of $\tilde{\zeta}_3$ is given by

$$\dot{\tilde{\zeta}}_3 = \dot{p}_{31}^\top p_{21} + p_{31}^\top \dot{p}_{21} = (u_1 - u_3)^\top p_{21} + p_{31}^\top (u_1 - u_2) \quad (34)$$

where (22a), (10a), and (7) were used. Similarly, the dynamics of $\tilde{\varphi}_3$ can be computed as

$$\begin{aligned} \dot{\tilde{\varphi}}_3 &= (u_1 - u_3)^\top (n_{123} \times p_{21}) + p_{31}^\top (\dot{n}_{123} \times p_{21}) \\ &\quad + p_{31}^\top (n_{123} \times (u_1 - u_2)). \end{aligned} \quad (35)$$

Therefore, the time derivative of (33a) is given by

$$\begin{aligned}\dot{W}_3 &= \tilde{\zeta}_3 \dot{\tilde{\zeta}}_3 + \tilde{\varphi}_3 \dot{\tilde{\varphi}}_3 \\ &= \tilde{\zeta}_3 [p_{21}^\top (u_1 - u_3) + p_{31}^\top (u_1 - u_2)] \\ &\quad + \tilde{\varphi}_3 [(n_{123} \times p_{21})^\top (u_1 - u_3) \\ &\quad + p_{31}^\top (\dot{n}_{123} \times p_{21}) + p_{31}^\top (n_{123} \times (u_1 - u_2))].\end{aligned}\quad (36)$$

Recall from Lemma 6 that $\dot{n}_{123} = 0$. Therefore, substituting $u_2 = 0$, $\|p_{21}\| = d_{21}$, (23a), and (23c) into (36) gives

$$\begin{aligned}\dot{W}_3 &= - [\tilde{\zeta}_3 p_{21}^\top + \tilde{\varphi}_3 (n_{123} \times p_{21})^\top] u_3 \\ &= -\mu_3 \tilde{\zeta}_3^2 d_{21}^2 - \nu_3 \tilde{\varphi}_3^2 \|n_{123} \times p_{21}\|^2\end{aligned}\quad (37)$$

where we used the fact that $p_{31} - p_{32} = p_{21}$. Since $\|n_{123}\| = 1$, then $\|n_{123} \times p_{21}\| = d_{21}$ and (37) becomes

$$\dot{W}_3 = -d_{21}^2 (\mu_3 \tilde{\zeta}_3^2 + \nu_3 \tilde{\varphi}_3^2), \quad (38)$$

which means $\tilde{\Lambda}_3 = 0$ is GES. \square

Lemma 9 *If $\|p_{ji}\| = d_{ji}$, $\|p_{ki}\| = d_{ki}$, $\|p_{kj}\| = d_{kj}$, and $u_i = u_j = u_k = 0$, then (23d) ensures that $\tilde{\Lambda}_l = [\tilde{\zeta}_l, \tilde{\varphi}_l, \tilde{\vartheta}_l] = 0$ is GES for the tetrahedron formed by agents $\{i, j, k, l\}$.*

Proof. The time derivative of (33b) along the dynamics of (22a), (22b), and (22c) is given by

$$\begin{aligned}\dot{W}_l &= \tilde{\zeta}_l [p_{ji}^\top (u_i - u_l) + p_{li}^\top (u_i - u_j)] \\ &\quad + \tilde{\varphi}_l [(u_i - u_l)^\top (n_{ijk} \times p_{ji}) + p_{li}^\top (\dot{n}_{ijk} \times p_{ji}) \\ &\quad + p_{li}^\top (n_{ijk} \times (u_i - u_j))] \\ &\quad + \tilde{\vartheta}_l [n_{ijk}^\top (u_i - u_l) + p_{li}^\top \dot{n}_{ijk}]\end{aligned}\quad (39)$$

where

$$\dot{n}_{ijk} = (u_i - u_k) \times p_{kj} + p_{ki} \times (u_j - u_k) \text{ if } \{i, j, k\} \neq \{1, 2, 3\},$$

and $\dot{n}_{123} = 0$ from Lemma 6.

After substituting $\|p_{ji}\| = d_{ji}$, $u_i = u_j = u_k = 0$, and (23d) into (39), we obtain

$$\begin{aligned}\dot{W}_l &= - [\tilde{\zeta}_l p_{ji}^\top + \tilde{\varphi}_l (n_{ijk} \times p_{ji})^\top + \tilde{\vartheta}_l n_{ijk}^\top] u_l \\ &= -\mu_l d_{ji}^2 \tilde{\zeta}_l^2 - \nu_l \tilde{\varphi}_l^2 \|n_{ijk} \times p_{ji}\|^2 - \lambda_l \tilde{\vartheta}_l^2 \|n_{ijk}\|^2\end{aligned}\quad (40)$$

where we used the fact that $p_{ji}^\top n_{ijk} = 0$. Given that $\|p_{ki}\| = d_{ki}$ and $\|p_{kj}\| = d_{kj}$, we know from (11) and

(18) that $\|n_{ijk}\|$ is constant. Therefore,

$$\dot{W}_l = -\mu_l d_{ji}^2 \tilde{\zeta}_l^2 - \nu_l d_{ji}^2 c \tilde{\varphi}_l^2 - \lambda_l c \tilde{\vartheta}_l^2 \quad (41)$$

where c is some positive constant. It then follows from (33b) and (41) that $[\tilde{\zeta}_l, \tilde{\varphi}_l, \tilde{\vartheta}_l] = 0$ is GES. \square

5.4 Main Results

The following two theorems give our main results.

Theorem 1 *Control (23) ensures $\tilde{\Lambda} = 0$ is GAS and $F(t) \rightarrow SCgt^3(F^*)$ as $t \rightarrow \infty$.*

Proof. We know from Lemma 7 that the subsystem composed of agents 1 and 2 is GES at $\tilde{\zeta}_2 = 0$. If a third agent is added to this subsystem, we get the cascade system

$$\dot{\tilde{\Lambda}}_3 = f_3(\tilde{\Lambda}_3, \tilde{\zeta}_2) \quad (42a)$$

$$\dot{\tilde{\zeta}}_2 = g_2(\tilde{\zeta}_2) \quad (42b)$$

where (42b) is in fact (32). If $\tilde{\zeta}_2 = 0$, then $u_2 = 0$ from (23b) and $\|p_{21}\| = d_{21}$ from (20) and (22a). Therefore, (42a) with $\tilde{\zeta}_2 = 0$ is GES at the origin by Lemma 8. It then follows from Lemma 2 that (42a) is ISS with respect to input $\tilde{\zeta}_2$. Finally, we can use Lemma 3 to show that the origin of (42), i.e., $[\tilde{\zeta}_2, \tilde{\Lambda}_3] = 0$, is GAS.

As we grow the graph step-by-step in the analysis by adding a vertex l with three outgoing edges to any distinct vertices i, j and k of the previous graph, we obtain the following cascade system at each step:

$$\dot{\tilde{\Lambda}}_l = f_l(\tilde{\Lambda}_l, z_{l-1}) \quad (43a)$$

$$\dot{z}_{l-1} = g_{l-1}(z_{l-1}) \quad (43b)$$

where $z_{l-1} = [\tilde{\Lambda}_2, \dots, \tilde{\Lambda}_{l-1}]$ and $i < j < k < l$. Note that the GAS of $z_{l-1} = 0$ for (43b) was established in the previous step. Therefore, we only need to check if (43a) is ISS with respect to input z_{l-1} . If $z_{l-1} = 0$, then $u_i = u_j = u_k = 0$ from (23d). Now, consider subframeworks $F_{l-1} = (G_{l-1}, p)$ and $F_{l-1}^* = (G_{l-1}, p^*)$ where G_{l-1} is the subgraph of G that contains vertices $\{1, \dots, l-1\}$ and the corresponding edges connecting these vertices in the original graph. The condition $z_{l-1} = 0$ is equivalent to $[\Lambda_2, \dots, \Lambda_{l-1}] = [\Lambda_2^*, \dots, \Lambda_{l-1}^*]$ where $\Lambda_i^* = \Lambda_i(\check{p}^*)$, and $\check{p}^* = [p_1^*, \dots, p_{l-1}^*]$. This indicates that F_{l-1} and F_{l-1}^* are strongly congruent from Lemma 4. Thus, we know $\|p_{ji}\| = d_{ji}$, $\|p_{ki}\| = d_{ki}$, and $\|p_{kj}\| = d_{kj}$ from Lemma 1. We can now use Lemma 9 to show that (43a) with $z_{l-1} = 0$ is GES at the origin. As a result, (43a)

is ISS by Lemma 2. Finally, we can invoke Lemma 3 to conclude that $\begin{bmatrix} z_{l-1}, \tilde{\Lambda}_l \end{bmatrix} = 0$ in (43) is GAS.

Repeating this process until $l = N$ leads to the conclusion that $\tilde{\Lambda} = 0$ is GAS, which implies $\Lambda(p(t)) \rightarrow \Lambda(p^*)$ as $t \rightarrow \infty$. Thus, we know from Lemma 4 that $F(t) \rightarrow \text{SCgt}^3(F^*)$ as $t \rightarrow \infty$. \square

Next, we show that the proposed control yields *local exponential* convergence to the equilibrium point. This property is important in practice since exponential stability is known to provide some level of robustness to the system (Khalil; 2015).

Theorem 2 *In the neighborhood of $\tilde{\Lambda} = 0$, the equilibrium point is locally exponentially stable (LES).*

Proof. The error dynamics for $\tilde{\Lambda}$ can be expressed as

$$\dot{\tilde{\Lambda}} = -A(\tilde{\Lambda})\tilde{\Lambda} \quad (44)$$

where

$$A(\tilde{\Lambda}) = \begin{bmatrix} D_1 & 0 & 0 & 0 & \cdots & \cdots & 0 \\ \star & D_2 & 0 & 0 & \cdots & \cdots & 0 \\ \star & 0 & D_3 & 0 & \cdots & \cdots & 0 \\ \star & \star & \star & D_4 & 0 & 0 & 0 \cdots & 0 \\ \star & \star & \star & 0 & D_5 & 0 & 0 \cdots & 0 \\ \star & \star & \star & 0 & 0 & D_6 & 0 \cdots & 0 \\ \vdots & & & & & \ddots & & \vdots \\ \star & \cdots & \cdots & \star & \star & 0 & 0 & 0 \\ \star & \cdots & \cdots & \star & 0 & \star & 0 & 0 \\ \star & \cdots & \cdots & \star & 0 & 0 & D_{3N-6} & 0 \end{bmatrix} \quad (45)$$

is a lower triangular $[3(N-3)+3] \times [3(N-3)+3]$ matrix whose diagonal elements are $D_1 = \mu_2$, $D_2 = \mu_3 \|p_{21}\|^2$, $D_3 = \nu_3 \|n_{123} \times p_{21}\|^2$, $D_4 = \mu_4 \|p_{21}\|^2$, $D_5 = \nu_4 \|n_{123} \times p_{21}\|^2$, $D_6 = \lambda_4 \|n_{123}\|^2$, \dots , $D_{3N-8} = \mu_N \|p_{N_1 N_2}\|^2$, $D_{3N-7} = \nu_N \|n_{N_1 N_2 N_3} \times p_{N_1 N_2}\|^2$, and $D_{3N-6} = \lambda_N \|n_{N_1 N_2 N_3}\|^2$ where N_1 , N_2 , and N_3 ($N_1 < N_2 < N_3$) are the out-neighbors of agent N .

Linearizing (44) at the equilibrium $\tilde{\Lambda} = 0$ yields

$$\dot{\tilde{\Lambda}} \approx -A(0)\tilde{\Lambda} \quad (46)$$

where $A(0)$ is a constant matrix whose eigenvalues (diagonal elements) are positive and can be made arbitrarily large by adjusting the control gains. Therefore, $\tilde{\Lambda} = 0$ is LES. \square

Remark 4 *It is worth noting that the 2D formation problem can be viewed as a degenerate case of the 3D problem. Specifically, we can consider the coordinates of agent i as $p_i = [x_i, y_i, 0]$ and express the control law with the third component equal to zero, i.e., $u_i = [u_{ix}, u_{iy}, 0]$. The results in Theorems 1 and 2 are also valid in the 2D case. This analysis is omitted here since it is based on similar arguments as above.*

6 Conclusion

This paper introduced a new set of controlled variables for avoiding undesirable equilibria in the 3D distance-based formation control approach. The proposed variables, which are related to the inter-agent distances, signed volume of the framework, and areas of the triangular faces, form an orthogonal basis that decomposes the control inputs into orthogonal subspaces. The resulting formation controller guarantees the global asymptotic stability and the local exponential stability of the desired formation shape with any initial conditions. This result is valid for any tetrahedralized-like framework with no conditions on the formation shape or control gains.

The proposed approach can also handle the 2D formation problem, unifying the two problems. Specifically, by setting the z -coordinate of each agent position to zero, we arrive at the orthogonal basis controller for 2D formations that appeared in our preliminary result in Liu, de Queiroz and Sahebsara (2020).

Appendix A Lemma Proofs

A.1 Lemma 1

Consider Figure 4 where $n_{123} = p_{23} \times p_{21}$ and $n_{124} = p_{24} \times p_{21}$ are the vectors normal to planes 1-2-3 and 1-2-4, respectively, and α is the dihedral angle between the two planes. Then, we have that

$$\begin{aligned} \cos \alpha &= \frac{n_{123}^\top n_{124}}{\|n_{123}\| \|n_{124}\|} \\ &= \frac{(p_{23} \times p_{21})^\top (p_{24} \times p_{21})}{\|p_{23}\| \|p_{21}\| \sin \theta_{123} \|p_{24}\| \|p_{21}\| \sin \theta_{124}} \end{aligned} \quad (47)$$

where θ_{ijk} is the face angle between edges (j, i) and (j, k) . Using property

$$(a \times b)^\top (c \times d) = (a^\top c)(b^\top d) - (a^\top d)(b^\top c), \quad (48)$$

we obtain

$$\begin{aligned}
& (p_{23} \times p_{21})^\top (p_{24} \times p_{21}) \\
&= (p_{23}^\top p_{24})(p_{21}^\top p_{21}) - (p_{23}^\top p_{21})(p_{21}^\top p_{24}) \\
&= \|p_{23}\| \|p_{24}\| \cos \theta_{423} \|p_{21}\|^2 \\
&\quad - \|p_{23}\| \|p_{21}\| \cos \theta_{123} \|p_{21}\| \|p_{24}\| \cos \theta_{124} \\
&= \|p_{21}\|^2 \|p_{23}\| \|p_{24}\| (\cos \theta_{423} - \cos \theta_{123} \cos \theta_{124}). \quad (49)
\end{aligned}$$

Substituting (49) into (47) gives

$$\cos \alpha = \frac{\cos \theta_{423} - \cos \theta_{123} \cos \theta_{124}}{\sin \theta_{123} \sin \theta_{124}}. \quad (50)$$

A dihedral angle α can be associated with the signed volume by defining a *signed dihedral angle*, α_s . To this end, given the tetrahedron in Figure 4, we can define its *signed height*, h , to have the same sign as the signed volume. Then,

$$\sin \alpha_s = \frac{h}{b} \quad (51)$$

where b is the distance from vertex 4 to edge (1, 2). Combining (50) and (51), we can calculate the signed dihedral angle as

$$\alpha_s = \arctan 2(h/b, \cos \alpha). \quad (52)$$

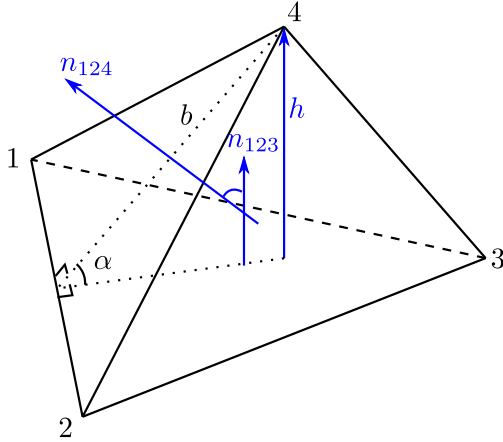


Fig. 4. Signed dihedral angle and signed height of a tetrahedron.

Now, we can prove Lemma 1 as follows.

(*Proof of \Rightarrow*) If F and \hat{F} are strongly congruent, then $\|p_i - p_j\| = \|\hat{p}_i - \hat{p}_j\|$, $\forall i, j \in \mathcal{V}$ and $\mathbf{V}(p) = \mathbf{V}(\hat{p})$ by definition. Therefore, since $\mathcal{E} \subset \mathcal{V} \times \mathcal{V}$, we know $\|p_i - p_j\| = \|\hat{p}_i - \hat{p}_j\|$, $\forall (i, j) \in \mathcal{E}$, i.e., F and \hat{F} are equivalent.

(*Proof of \Leftarrow*) If $|\mathcal{V}| = 4$, then framework equivalency and congruency are equivalent, so the conditions for strong congruency are trivially satisfied.

If a vertex is added such that $|\mathcal{V}| = 5$, the resulting 3D framework will have three additional edges and one additional tetrahedron. Consider without loss of generality the framework in Figure 5, and denote the signed dihedral angle between planes 1-2-3 and 1-2-4 as α_{s1} and between planes 1-2-3 and 1-2-5 as α_{s2} . Then, the signed dihedral angle between planes 1-2-4 and 1-2-5 is $\alpha_{s3} = \alpha_{s1} + \alpha_{s2}$.

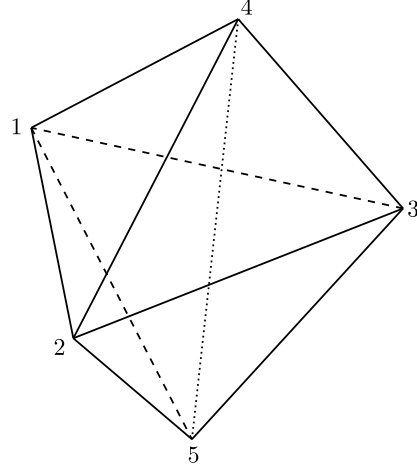


Fig. 5. Framework with $|\mathcal{V}| = 5$ containing two tetrahedrons.

Since F and \hat{F} are equivalent, $\|p_i - p_j\| = \|\hat{p}_i - \hat{p}_j\|$, $\forall (i, j) \in \mathcal{E}$. This along with $\mathbf{V}(p) = \mathbf{V}(\hat{p})$ indicates that all face angles in F and \hat{F} are equal. From (52), we then know that $\alpha_{s1} = \hat{\alpha}_{s1}$, $\alpha_{s2} = \hat{\alpha}_{s2}$, and $\alpha_{s3} = \hat{\alpha}_{s3}$ where $\hat{\alpha}_{si}$ denotes the i th dihedral angle of \hat{F} . Using (50), we have

$$\cos \alpha_{s3} = \frac{\cos \theta_{425} - \cos \theta_{124} \cos \theta_{125}}{\sin \theta_{124} \sin \theta_{125}}. \quad (53)$$

Since $\alpha_{s3}(p) = \alpha_{s3}(\hat{p})$ and all face angles are equal, we obtain

$$\cos \theta_{425} = \cos \hat{\theta}_{425}. \quad (54)$$

After applying (54) to the law of cosines, we arrive at $\|p_5 - p_4\| = \|\hat{p}_5 - \hat{p}_4\|$. This proves that $\|p_i - p_j\| = \|\hat{p}_i - \hat{p}_j\|$, $\forall i, j \in \mathcal{V}$, so F and \hat{F} are strongly congruent for $|\mathcal{V}| = 5$.³

As more vertices are added, each new vertex will create a new tetrahedron. Thus, the above process can be recursively employed to show that F and \hat{F} are strongly congruent for $|\mathcal{V}| = N$.

³ This analysis is not restricted to convex structures such as Figure 5. A similar analysis can be applied to concave cases.

A.2 Lemma 4

(Proof of \Rightarrow) From (20), (10a), and the fact that strong congruency implies $\|p_{ij}\| = \|\hat{p}_{ij}\| \forall i, j \in \mathcal{V}$, we have

$$\zeta_2(p) = \|p_{21}\| = \|\hat{p}_{21}\| = \zeta_2(\hat{p}) \quad (55)$$

and

$$\begin{aligned} \zeta_3(p) &= p_{31}^\top p_{21} = \|p_{31}\| \|p_{21}\| \frac{\|p_{31}\|^2 + \|p_{21}\|^2 - \|p_{32}\|^2}{2 \|p_{31}\| \|p_{21}\|} \\ &= \frac{\|p_{31}\|^2 + \|p_{21}\|^2 - \|p_{32}\|^2}{2} \\ &= \frac{\|\hat{p}_{31}\|^2 + \|\hat{p}_{21}\|^2 - \|\hat{p}_{32}\|^2}{2} = \zeta_3(\hat{p}). \end{aligned} \quad (56)$$

From (15) and (18), we obtain

$$\begin{aligned} \varphi_3(p) &= n_{123}^\top (p_{31} \times p_{32}) = \|p_{31} \times p_{32}\| = 2\check{S}_{123}(p) \\ &= \frac{1}{2} \left(2 \|p_{21}\|^2 \|p_{32}\|^2 + 2 \|p_{31}\|^2 \|p_{32}\|^2 - \|p_{21}\|^4 \right. \\ &\quad \left. - \|p_{31}\|^4 - \|p_{32}\|^4 + 2 \|p_{21}\|^2 \|p_{31}\|^2 \right)^{1/2} \\ &= \frac{1}{2} \left(2 \|\hat{p}_{21}\|^2 \|\hat{p}_{32}\|^2 + 2 \|\hat{p}_{31}\|^2 \|\hat{p}_{32}\|^2 - \|\hat{p}_{21}\|^4 \right. \\ &\quad \left. - \|\hat{p}_{31}\|^4 - \|\hat{p}_{32}\|^4 + 2 \|\hat{p}_{21}\|^2 \|\hat{p}_{31}\|^2 \right)^{1/2} \\ &= 2\check{S}_{123}(\hat{p}) = \varphi_3(\hat{p}). \end{aligned} \quad (57)$$

The relation $\zeta_4(p) = \zeta_4(\hat{p})$ can be shown as in (56). From (10b), (11), and (18), we get

$$\begin{aligned} \varphi_4(p) &= n_{123}^\top (p_{21} \times p_{41}) \\ &= \left(\frac{p_{31} \times p_{32}}{\|p_{31} \times p_{32}\|} \right)^\top (p_{21} \times p_{41}) \\ &= \frac{1}{\|p_{31} \times p_{32}\|} (-p_{32} \times p_{31})^\top (-p_{41} \times p_{21}) \\ &= \frac{1}{\|p_{31} \times p_{32}\|} [(-p_{32} \times p_{32} - p_{32} \times p_{21})^\top (-p_{42} \times p_{21} \\ &\quad - p_{21} \times p_{21})] \\ &= \frac{1}{\|p_{31} \times p_{32}\|} (p_{32} \times p_{12})^\top (p_{42} \times p_{12}) \\ &= \frac{1}{2\check{S}_{123}(p)} [(p_{32})^\top p_{42} (p_{12})^\top p_{12} - (p_{32})^\top p_{12} (p_{12})^\top p_{42}] \\ &= \frac{1}{2\check{S}_{123}(p)} \left[\|p_{32}\| \|p_{42}\| \frac{\|p_{32}\|^2 + \|p_{42}\|^2 - \|p_{43}\|^2}{2 \|p_{32}\| \|p_{42}\|} \|p_{12}\|^2 \right. \\ &\quad \left. - \|p_{32}\| \|p_{12}\| \frac{\|p_{32}\|^2 + \|p_{12}\|^2 - \|p_{13}\|^2}{2 \|p_{32}\| \|p_{12}\|} \right. \\ &\quad \left. \cdot \|p_{12}\| \|p_{42}\| \frac{\|p_{12}\|^2 + \|p_{42}\|^2 - \|p_{41}\|^2}{2 \|p_{12}\| \|p_{42}\|} \right]. \end{aligned} \quad (58)$$

Since (58) is only a function of the inter-agent distances, then $\varphi_4(p) = \varphi_4(\hat{p})$. A useful formula for calculating the signed volume V_{ijkl} is given by the Cayley-Menger determinant (Sommerville; 2011):

$$V_{ijkl} = \pm \sqrt{\frac{1}{288} \begin{vmatrix} 0 & 1 & 1 & 1 & 1 \\ 1 & 0 & \|p_{ji}\|^2 & \|p_{ki}\|^2 & \|p_{li}\|^2 \\ 1 & \|p_{ji}\|^2 & 0 & \|p_{kj}\|^2 & \|p_{lj}\|^2 \\ 1 & \|p_{ki}\|^2 & \|p_{kj}\|^2 & 0 & \|p_{lk}\|^2 \\ 1 & \|p_{li}\|^2 & \|p_{lj}\|^2 & \|p_{lk}\|^2 & 0 \end{vmatrix}}, \quad (59)$$

where the sign convention described in Section 2.2 determines if the sign is positive or negative. From (17), we have $\vartheta_4(p) = -3V_{1234}(p)/\check{S}_{123}(p)$. Given (18) and (59), we can see that $\vartheta_4(p)$ is only dependent on the inter-agent distances and the sign of the volume; hence, it is clear that $\vartheta_4(p) = \vartheta_4(\hat{p})$.

Repeating this analysis for ζ_l , φ_l , and ϑ_l , $l = 5, \dots, N$ leads to the conclusion that $\Lambda(p) = \Lambda(\hat{p})$.

(Proof of \Leftarrow) If $\Lambda(p) = \Lambda(\hat{p})$, then $\zeta_l(p) = \zeta_l(\hat{p})$, $l = 2, \dots, N$, $\varphi_l(p) = \varphi_l(\hat{p})$, $l = 3, \dots, N$, and $\vartheta_l(p) = \vartheta_l(\hat{p})$, $l = 4, \dots, N$. From $\zeta_2(p) = \zeta_2(\hat{p})$, we obtain

$$\|p_{21}\| = \|\hat{p}_{21}\| \quad (60)$$

where (20) was used. From $\zeta_3(p) = \zeta_3(\hat{p})$ and (10a), we have

$$\begin{aligned} &\|p_{31}\| \|p_{21}\| \frac{\|p_{31}\|^2 + \|p_{21}\|^2 - \|p_{32}\|^2}{2 \|p_{31}\| \|p_{21}\|} \\ &= \frac{\|p_{31}\|^2 + \|p_{21}\|^2 - \|p_{32}\|^2}{2} \\ &= \frac{\|\hat{p}_{31}\|^2 + \|\hat{p}_{21}\|^2 - \|\hat{p}_{32}\|^2}{2} \end{aligned} \quad (61)$$

where the law of cosines were used. This leads to

$$\|p_{31}\|^2 + \|p_{21}\|^2 - \|p_{32}\|^2 = \|\hat{p}_{31}\|^2 + \|\hat{p}_{21}\|^2 - \|\hat{p}_{32}\|^2. \quad (62)$$

From $\varphi_3(p) = \varphi_3(\hat{p})$ and (15), we get

$$\check{S}_{123}(p) = \check{S}_{123}(\hat{p}). \quad (63)$$

Applying (18) to (63) yields

$$\begin{aligned} &2 \|p_{21}\|^2 \|p_{31}\|^2 + 2 \|p_{21}\|^2 \|p_{32}\|^2 + 2 \|p_{31}\|^2 \|p_{32}\|^2 \\ &\quad - \|p_{21}\|^4 - \|p_{31}\|^4 - \|p_{32}\|^4 \\ &= 2 \|\hat{p}_{21}\|^2 \|\hat{p}_{31}\|^2 + 2 \|\hat{p}_{21}\|^2 \|\hat{p}_{32}\|^2 + 2 \|\hat{p}_{31}\|^2 \|\hat{p}_{32}\|^2 \\ &\quad - \|\hat{p}_{21}\|^4 - \|\hat{p}_{31}\|^4 - \|\hat{p}_{32}\|^4. \end{aligned} \quad (64)$$

Combining (60), (62), and (64) gives $\|p_{31}\| = \|\hat{p}_{31}\|$ and $\|p_{32}\| = \|\hat{p}_{32}\|$.

Next, from $\zeta_4(p) = \zeta_4(\hat{p})$, $\varphi_4(p) = \varphi_4(\hat{p})$, and $\vartheta_4(p) = \vartheta_4(\hat{p})$, we get

$$\|p_{41}\|^2 + \|p_{21}\|^2 - \|p_{42}\|^2 = \|\hat{p}_{41}\|^2 + \|\hat{p}_{21}\|^2 - \|\hat{p}_{42}\|^2, \quad (65)$$

$$\begin{aligned} & -\|p_{21}\|^4 + \|p_{21}\|^2 \|p_{31}\|^2 + \|p_{21}\|^2 \|p_{32}\|^2 + \|p_{21}\|^2 \|p_{41}\|^2 \\ & + \|p_{21}\|^2 \|p_{42}\|^2 - 2 \|p_{43}\|^2 \|p_{21}\|^2 - \|p_{31}\|^2 \|p_{41}\|^2 \\ & + \|p_{31}\|^2 \|p_{42}\|^2 + \|p_{32}\|^2 \|p_{41}\|^2 - \|p_{32}\|^2 \|p_{42}\|^2 \\ & = -\|\hat{p}_{21}\|^4 + \|\hat{p}_{21}\|^2 \|\hat{p}_{31}\|^2 + \|\hat{p}_{21}\|^2 \|\hat{p}_{32}\|^2 + \|\hat{p}_{21}\|^2 \|\hat{p}_{41}\|^2 \\ & + \|\hat{p}_{21}\|^2 \|\hat{p}_{42}\|^2 - 2 \|\hat{p}_{43}\|^2 \|\hat{p}_{21}\|^2 - \|\hat{p}_{31}\|^2 \|\hat{p}_{41}\|^2 \\ & + \|\hat{p}_{31}\|^2 \|\hat{p}_{42}\|^2 + \|\hat{p}_{32}\|^2 \|\hat{p}_{41}\|^2 - \|\hat{p}_{32}\|^2 \|\hat{p}_{42}\|^2, \end{aligned} \quad (66)$$

and

$$\begin{aligned} & \begin{vmatrix} 0 & 1 & 1 & 1 & 1 \\ 1 & 0 & \|p_{21}\|^2 & \|p_{31}\|^2 & \|p_{41}\|^2 \\ 1 & \|p_{21}\|^2 & 0 & \|p_{32}\|^2 & \|p_{42}\|^2 \\ 1 & \|p_{31}\|^2 & \|p_{32}\|^2 & 0 & \|p_{43}\|^2 \\ 1 & \|p_{41}\|^2 & \|p_{42}\|^2 & \|p_{43}\|^2 & 0 \end{vmatrix} \\ & = \begin{vmatrix} 0 & 1 & 1 & 1 & 1 \\ 1 & 0 & \|\hat{p}_{21}\|^2 & \|\hat{p}_{31}\|^2 & \|\hat{p}_{41}\|^2 \\ 1 & \|\hat{p}_{21}\|^2 & 0 & \|\hat{p}_{32}\|^2 & \|\hat{p}_{42}\|^2 \\ 1 & \|\hat{p}_{31}\|^2 & \|\hat{p}_{32}\|^2 & 0 & \|\hat{p}_{43}\|^2 \\ 1 & \|\hat{p}_{41}\|^2 & \|\hat{p}_{42}\|^2 & \|\hat{p}_{43}\|^2 & 0 \end{vmatrix} \end{aligned} \quad (67)$$

Since we know that $\|p_{21}\| = \|\hat{p}_{21}\|$, $\|p_{31}\| = \|\hat{p}_{31}\|$, and $\|p_{32}\| = \|\hat{p}_{32}\|$, we can use (65), (66), and (67) to show $\|p_{41}\| = \|\hat{p}_{41}\|$, $\|p_{42}\| = \|\hat{p}_{42}\|$, and $\|p_{43}\| = \|\hat{p}_{43}\|$.

Repeating the same analysis on ζ_l , φ_l , and ϑ_l , $l = 5, \dots, N$ gives $\mathbf{V}(p) = \mathbf{V}(\hat{p})$ and $\gamma(p) = \gamma(\hat{p})$. Then, by Lemma 1, we know F and \hat{F} are strongly congruent.

A.3 Lemma 5

Since agents i , j , and k are located at their desired inter-agent distances, we can let $p_i = [-d_{ji}/2, 0, 0]$, $p_j = [d_{ji}/2, 0, 0]$, $p_k = [x_k, y_k, 0]$, and $p_l = [x_l, y_l, z_l]$ without the loss of generality. We also assume $y_k > 0$ for simplicity. From the above coordinates, we get

$$\|p_{li}\|^2 = \left(x_l + \frac{d_{ji}}{2}\right)^2 + y_l^2 + z_l^2 \quad (68)$$

$$\|p_{lj}\|^2 = \left(x_l - \frac{d_{ji}}{2}\right)^2 + y_l^2 + z_l^2. \quad (69)$$

After solving for x_l , we arrive at

$$x_l = \frac{\|p_{li}\|^2 - \|p_{lj}\|^2}{2d_{ji}}. \quad (70)$$

When $\tilde{\zeta}_l = 0$, we know from (10a) and (22a) that $\|p_{li}\|^2 - \|p_{lj}\|^2 = d_{li}^2 - d_{lj}^2$. Substituting this into (70) gives

$$x_l = \frac{d_{li}^2 - d_{lj}^2}{2d_{ji}}. \quad (71)$$

This means that all points satisfying $\tilde{\zeta}_l = 0$ lie on the plane defined by (71) (blue plane in Figure 6), which is normal to vector p_{ji} .

Now, substituting the known coordinates of p_i , p_j , p_k , and p_l into (10b) yields

$$\varphi_l = d_{ji} \|n_{ijk}^*\| y_l \quad (72)$$

where $n_{ijk}^* := n_{ijk}(p^*)$ and

$$\|n_{ijk}^*\| = \begin{cases} \|p_{ki}^* \times p_{kj}^*\| & \text{if } \{i, j, k\} \neq \{1, 2, 3\} \\ 1 & \text{if } \{i, j, k\} = \{1, 2, 3\}. \end{cases}$$

When $\tilde{\varphi}_l = 0$, we have from (72) and (22b) that

$$y_l = \frac{\varphi_l^*}{d_{ji} \|n_{ijk}^*\|}. \quad (73)$$

This indicates that all the points satisfying $\tilde{\varphi}_l = 0$ lie on the plane defined by (73) (red plane in Figure 6), which is orthogonal to plane $\tilde{\zeta}_l = 0$.

Finally, we can use (10c) and (79) to write

$$\vartheta_l = p_{li}^\top \frac{n_{ijk}}{\|n_{ijk}\|} \|n_{ijk}\| = p_{li}^\top \frac{p_{ki} \times p_{kj}}{\|p_{ki} \times p_{kj}\|} \|n_{ijk}\|. \quad (74)$$

From the known coordinates of p_i , p_j , p_k , and p_l , we obtain $p_{li}^\top (p_{ki} \times p_{kj}) = -z_l \|n_{ijk}\|$. Since $\|p_{ji}\| = d_{ji}$, $\|p_{ki}\| = d_{ki}$, and $\|p_{kj}\| = d_{kj}$, we get from (11) that $\|n_{ijk}\| = \|n_{ijk}^*\|$. Therefore, (74) simplifies to

$$\vartheta_l = -\|n_{ijk}^*\| z_l. \quad (75)$$

When $\tilde{\vartheta}_l = 0$, we can use (22c) and (75) to get

$$z_l = -\frac{\vartheta_l^*}{\|n_{ijk}^*\|}. \quad (76)$$

That is, all the points satisfying $\tilde{\vartheta}_l = 0$ are on the plane defined by (76) (green plane in Figure 6), which is orthogonal to planes $\tilde{\zeta}_l = 0$ and $\tilde{\varphi}_l = 0$.

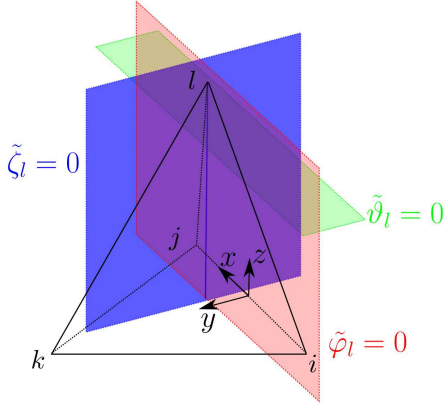


Fig. 6. Graphical representation of projection errors: Points on the blue plane satisfy $\tilde{\zeta}_l = 0$; points on the red plane satisfy $\tilde{\varphi}_l = 0$; points on the green plane satisfy $\tilde{\vartheta}_l = 0$.

Appendix B Desired Projection Variables

In the following, we show how the desired values for the 3D projection variables can be computed in terms of the desired inter-agent distances.

First, we have from (10a) that

$$\begin{aligned} \zeta_l^* &= (p_{li}^*)^\top p_{ji}^* \\ &= \|p_{li}^*\| \|p_{ji}^*\| \frac{\|p_{li}^*\|^2 + \|p_{ji}^*\|^2 - \|p_{lj}^*\|^2}{2 \|p_{li}^*\| \|p_{ji}^*\|} \\ &= \frac{d_{li}^2 + d_{ji}^2 - d_{lj}^2}{2}. \end{aligned} \quad (77)$$

Next, from (10b):

$$\begin{aligned} \varphi_l^* &= (p_{li}^*)^\top (n_{ijk}^* \times p_{ji}^*) = (n_{ijk}^*)^\top (p_{ji}^* \times p_{li}^*) \\ &= \|n_{ijk}^*\| \frac{(n_{ijk}^*)^\top}{\|n_{ijk}^*\|} (p_{ji}^* \times p_{li}^*). \end{aligned} \quad (78)$$

Notice from (11) that

$$\frac{n_{ijk}^*}{\|n_{ijk}^*\|} = \frac{p_{ki}^* \times p_{kj}^*}{\|p_{ki}^* \times p_{kj}^*\|} \quad (79)$$

for both $\{i, j, k\} \neq \{1, 2, 3\}$ and $\{i, j, k\} = \{1, 2, 3\}$. Af-

ter applying (79) to (78), we obtain

$$\varphi_l^* = \frac{\|n_{ijk}^*\|}{\|p_{ki}^* \times p_{kj}^*\|} (p_{ki}^* \times p_{kj}^*)^\top (p_{ji}^* \times p_{li}^*). \quad (80)$$

From (11),

$$\frac{\|n_{ijk}^*\|}{\|p_{ki}^* \times p_{kj}^*\|} = \begin{cases} 1 & \text{if } \{i, j, k\} \neq \{1, 2, 3\} \\ \frac{1}{\|p_{31}^* \times p_{32}^*\|} & \text{if } \{i, j, k\} = \{1, 2, 3\}. \end{cases} \quad (81)$$

Given (18) and the fact that $\|p_{ji}^*\| = d_{ji}$, $\forall (j, i) \in \mathcal{E}$, it is obvious that (81) is only dependent on the desired distances. Now,

$$\begin{aligned} & (p_{ki}^* \times p_{kj}^*)^\top (p_{ji}^* \times p_{li}^*) \\ &= (-p_{kj}^* \times p_{ki}^*)^\top (-p_{li}^* \times p_{ji}^*) \\ &= (-p_{kj}^* \times p_{ki}^* - p_{kj}^* \times p_{ji}^*)^\top (-p_{li}^* \times p_{ji}^* - p_{ji}^* \times p_{li}^*) \\ &= (p_{kj}^* \times p_{ji}^*)^\top (p_{lj}^* \times p_{ij}^*) \\ &= \|p_{kj}^*\| \|p_{lj}^*\| \frac{\|p_{kj}^*\|^2 + \|p_{lj}^*\|^2 - \|p_{lk}^*\|^2}{2 \|p_{kj}^*\| \|p_{lj}^*\|} \|p_{ij}^*\|^2 \\ &\quad - \|p_{kj}^*\| \|p_{ij}^*\| \frac{\|p_{kj}^*\|^2 + \|p_{ij}^*\|^2 - \|p_{ik}^*\|^2}{2 \|p_{kj}^*\| \|p_{ij}^*\|} \\ &\quad \cdot \|p_{ij}^*\| \|p_{lj}^*\| \frac{\|p_{ij}^*\|^2 + \|p_{lj}^*\|^2 - \|p_{li}^*\|^2}{2 \|p_{ij}^*\| \|p_{lj}^*\|}, \end{aligned} \quad (82)$$

which is also only dependent on the desired distances. Thus, (80) is only a function of d_{ji} , $\forall (j, i) \in \mathcal{E}$.

Finally, it follows from (10c) that

$$\vartheta_l^* = (p_{li}^*)^\top n_{ijk}^* = (p_{li}^*)^\top n_{ijk}^* - (p_{ki}^*)^\top n_{ijk}^* = (p_{lk}^*)^\top n_{ijk}^*. \quad (83)$$

If $\{i, j, k\} \neq \{1, 2, 3\}$, then from (11)

$$\begin{aligned} \vartheta_l^* &= (p_{lk}^*)^\top (p_{ki}^* \times p_{kj}^*) \\ &= (p_{lk}^*)^\top [(p_{li}^* - p_{lk}^*) \times (p_{lj}^* - p_{lk}^*)] \\ &= (p_{lk}^*)^\top (p_{li}^* \times p_{lj}^* - p_{li}^* \times p_{lk}^* - p_{lk}^* \times p_{lj}^* + p_{lk}^* \times p_{lk}^*) \\ &= (p_{lk}^*)^\top (p_{li}^* \times p_{lj}^*) = -6V_{ijkl}^* \end{aligned} \quad (84)$$

where $V_{ijkl}^* := V(p_i^*, p_j^*, p_k^*, p_l^*)$ from (2). Note that V_{ijkl}^* can be calculated using (59) with $\|p_{ji}^*\| = d_{ji}$ where the sign is based on the desired ordering of vertices i, j, k per the convention described in Section 2.2. If $\{i, j, k\} = \{1, 2, 3\}$, then from (11) and the calculations in (84), we arrive at

$$\vartheta_l^* = -\frac{6V_{123l}^*}{\|p_{31}^* \times p_{32}^*\|} \quad (85)$$

where (18) is used to calculate the denominator in terms of the desired distances.

The desired projections ζ_2^* , ζ_3^* , and φ_3^* are special cases of the above variables. From (12), we have that

$$\zeta_2^* = (p_{21}^*)^\top \frac{p_{21}^*}{\|p_{21}^*\|} = \|p_{21}^*\| = d_{21}. \quad (86)$$

From (14) and (77), we obtain

$$\zeta_3^* = (p_{31}^*)^\top p_{21}^* = \frac{d_{31}^2 + d_{21}^2 - d_{32}^2}{2}.$$

Finally, from (15), we have

$$\begin{aligned} \varphi_3^* &= (p_{31}^*)^\top (n_{123}^* \times p_{21}^*) = (n_{123}^*)^\top (p_{31}^* \times p_{32}^*) \\ &= \|p_{31}^* \times p_{32}^*\| = 2\check{S}_{123}^* \end{aligned} \quad (87)$$

where $\check{S}_{123}^* := \check{S}_{123}(p_{31}^*, p_{32}^*)$ from (18) is only dependent on the desired distances.

References

- Anderson, B., Sun, Z., Sugie, T., Azuma, S. and Sakurama, K. (2017). Formation shape control with distance and area constraints, *IFAC Journal of Systems and Control* **1**: 2–12.
- Anderson, B., Yu, C., Fidan, B. and Hendrickx, J. M. (2008). Rigid graph control architectures for autonomous formations, *IEEE Control Systems* **28**(6).
- Asimow, L. and Roth, B. (1979). The rigidity of graphs, II, *Journal of Mathematical Analysis and Applications* **68**(1): 171–190.
- Cao, Y., Sun, Z., Anderson, B. and Sugie, T. (2019). Almost global convergence for distance-and area-constrained hierarchical formations without reflection, *IEEE 15th International Conference on Control and Automation*, pp. 1534–1539.
- de Queiroz, M., Cai, X. and Feemster, M. (2019). *Formation Control of Multi-agent Systems: A Graph Rigidity Approach*, Hoboken, NJ: Wiley.
- Eren, T., Whiteley, W., Anderson, B., Morse, A. S. and Belhumeur, P. N. (2005). Information structures to secure control of rigid formations with leader-follower architecture, *Proceedings of the American Control Conference, 2005.*, IEEE, pp. 2966–2971.
- Ferreira-Vazquez, E. D., Flores-Godoy, J. J., Hernandez-Martinez, E. G. and Fernandez-Anaya, G. (2016). Adaptive control of distance-based spatial formations with planar and volume restrictions, *2016 IEEE Conference on Control Applications*, Buenos Aires, Argentina, pp. 905–910.
- Ferreira-Vazquez, E. D., Hernandez-Martinez, E. G., Flores-Godoy, J. J., Fernandez-Anaya, G. and Paniagua-Contro, P. (2016). Distance-based formation control using angular information between robots, *Journal of Intelligent & Robotic Systems* **83**(3-4): 543–560.
- Grasegger, G., Koutschan, C. and Tsigaridas, E. (2018). Lower bounds on the number of realizations of rigid graphs, *Experimental Mathematics* **64****58**: 1–12. DOI:10.1080/10586458.2018.1437851.
- Izmestiev, I. (2009). Infinitesimal rigidity of frameworks and surfaces, *Lectures on Infinitesimal Rigidity, Kyushu University, Japan*.
- Jackson, B. (2007). Notes on the rigidity of graphs, *Levico Conference Notes*, Vol. 4.
- Jing, G. and Wang, L. (2020). Multiagent flocking with angle-based formation shape control, *IEEE Transactions on Automatic Control* **65**(2): 817–823.
- Kang, S., Park, M. and Ahn, H. (2017). Distance-based cycle-free persistent formation: Global convergence and experimental test with a group of quadcopters, *IEEE Transactions on Industrial Electronics* **64**(1): 380–389.
- Khalil, H. K. (2015). *Nonlinear Control*, Pearson New York.
- Krick, L., Broucke, M. E. and Francis, B. A. (2009). Stabilisation of infinitesimally rigid formations of multi-robot networks, *International Journal of Control* **82**(3): 423–439.
- Lan, X., Xu, W. and Wei, Y. (2018). Adaptive 3D distance-based formation control of multiagent systems with unknown leader velocity and coplanar initial positions, *Complexity*. Article ID 1814653.
- Liu, T. and de Queiroz, M. (n.d.). Distance + angle-based control of 2d rigid formations, *IEEE Transactions on Cybernetics*. DOI:10.1109/TCYB.2020.2973592, in press.
- Liu, T., de Queiroz, M. and Sahebsara, F. (2020). Distance-based planar formation control using orthogonal variables, *IEEE Conference on Control Technology and Applications*, Montreal, Canada, pp. 64–69.
- Liu, T., de Queiroz, M., Zhang, P. and Khaledyan, M. (n.d.). Further results on the distance and area control of planar formations, *International Journal of Control*. DOI:10.1080/00207179.2019.1616824, in press.
- Liu, T., Fernández-Kim, V. and de Queiroz, M. (2020). Switching formation shape control with distance+ area/angle feedback, *Systems & Control Letters* **135**. Article 104598.
- Mallison, H. V. (1935). The use of signs in geometry, *The Mathematical Gazette* **19**(233): 124–130. URL: <http://www.jstor.org/stable/3608027>
- Mou, S., Cao, M. and Morse, A. S. (2015). Target-point formation control, *Automatica* **61**: 113–118.
- Oh, K., Park, M. and Ahn, H. (2015). A survey of multi-agent formation control, *Automatica* **53**: 424–440.
- Sommerville, D. (2011). *An Introduction to the Geometry of N Dimensions*, New Academic Science.
- Sugie, T., Anderson, B., Sun, Z. and Dong, H. (2018). On a hierarchical control strategy for multi-agent formation without reflection, *2018 IEEE Conference on Decision and Control*, pp. 2023–2028.
- Summers, T. H., Yu, C., Dasgupta, S. and Anderson, B.

- (2011). Control of minimally persistent leader-remote-follower and coleader formations in the plane, *IEEE Transactions on Automatic Control* **56**(12): 2778–2792.
- Yu, C., Hendrickx, J. M., Fidan, B., Anderson, B. and Blondel, V. D. (2007). Three and higher dimensional autonomous formations: Rigidity, persistence and structural persistence, *Automatica* **43**(3): 387–402.
- Zwillinger, D. (2002). *CRC Standard Mathematical Tables and Formulae*, 31st edn, CRC Press.